

GMPLS Control Plane Network Design With Resilience Guarantees

Marc Ruiz, Jordi Perelló, Luis Velasco, Salvatore Spadaro, Jaume Comellas, and Gabriel Junyent

Abstract—A one-to-one association between data and control channels has traditionally existed in transport networks. Being the control plane embedded in the data plane, the design of the former, as well as its resilience, has been addressed in the latter's one. However, a main GMPLS architectural requirement is to provide a clean separation between control and data planes. In this sense, the control plane in GMPLS networks may describe a different topology than the data plane, even realized over a separated IP network. As a consequence of this, data and control network design become no more linked in such scenarios. To the best of our knowledge, no works in the literature have addressed an independent design of the control plane in GMPLS-enabled networks regardless of the data plane. In this paper, we provide a method to obtain the optimal GMPLS control plane design, minimizing the network Capital Expenditures (CAPEX) while matching specific resilience requirements. To this goal, the problem of finding an optimal control plane topology that ensures a certain resilience level is formulated as a non-linear combinatorial model. This model, however, does not scale properly for large backbone networks. In view of this, a constructive linear method is also presented and its optimality validated through simulations on several reference network scenarios. Furthermore, its benefits in terms of total execution time are also highlighted.

Index Terms—ASON, GMPLS, control plane network design, network costs minimization, mathematical programming, survivable networks.

I. INTRODUCTION

CURRENT transport network operation relies on three clearly separated planes, providing each one different functionalities. From the bottom to the top of the network architecture, we find the data, control and management planes. The data plane represents those physical network resources that support the exchange of information between end-users (e.g., end-to-end connections). The control plane is devoted to automate the routing and signaling of the paths whereby the end-user data will flow. The goal of the control plane is the provisioning of advanced network services such as Bandwidth on Demand (BoD) to support short-term and long-term traffic

Manuscript received January 15, 2010; revised July 22, 2010, September 30, 2010; accepted October 22, 2010. Date of publication November 09, 2010; date of current version December 17, 2010. This work was supported in part by the BONE project ("Building the Future Optical Network in Europe"), a Network of Excellence funded by the European Commission through the 7th ICT-Framework Program, and in part by the Spanish Science Ministry through the TEC2008-02634 ENGINE project.

The authors are with the Advanced Broadband Communications Center (CCABA), Universitat Politècnica de Catalunya (UPC), Barcelona, Spain (e-mail: mruiz@ac.upc.edu; perello@ac.upc.edu; lvelasco@ac.upc.edu; spadaro@tsc.upc.edu; comellas@tsc.upc.edu; junyent@tsc.upc.edu).

Color versions of one or more of the figures in this paper are available online at <http://ieeexplore.ieee.org>.

Digital Object Identifier 10.1109/JLT.2010.2090648

fluctuations efficiently [1]. On top, the management plane supervises the whole network operation.

Typically, a logical separation has been only introduced between end-user, control and management information, still sharing the same transmission medium. For example, SONET/SDH networks [2] use the Data Communications Channel (DCC) bytes in the regenerator and multiplex sections to create *in-band* control channels. Similarly, control packets are transmitted *in-band* together with end-user data packets in MPLS networks [3]. This makes the separation of the data and the control plane difficult¹, as they remain intrinsically associated. Moreover, no room is left for a more efficient control plane design or the proposal of protection and restoration schemes different than those of the data plane.

In this context, the Automatically Switched Optical Network (ASON, [4]) has been adopted as the leading architecture towards flexible and easy-to-maintain optical transport networks. Basically, ASON describes the reference architecture for the control plane and its interfaces. It is worth mentioning, however, that all specifications in [4] are technology-independent. In particular, the Generalized Multi-Protocol Label Switching (GMPLS, [5]) technology has arisen as the most accepted solution for implementing the control plane functionalities in ASON. This leads to the term ASON/GMPLS, referring to a GMPLS-controlled ASON.

Essentially, GMPLS is a set of IP protocols defined by the Internet Engineering Task Force (IETF). These protocols are an extension of the existing ones in MPLS, allowing the management of different switching capabilities in an integrated way. In fact, not only Packet Switched Capable (PSC) interfaces can be managed (as in MPLS), but also Time-Division Multiplexing Capable (TDMC), Lambda Switched Capable (LSC) or even Fiber Switched Capable (FSC) ones. In order to achieve this, GMPLS proposes the use of RSVP-TE for signaling [6], OSPF-TE for routing [7] and a new protocol called Link Management Protocol (LMP) for resource management [8].

As mentioned in [9], the control and the data plane in all-optical networks (e.g., composed of LSC interfaces) are not as tightly coupled as in MPLS or SONET/SDH. In fact, they do not even permit an *in-band* control plane configuration. As end-to-end connections optically bypass all intermediate nodes from source to destination, no control information can be terminated there.

In light of this, a separation between control and data planes was introduced in GMPLS, letting the control information to be transmitted on a different wavelength of the same fiber (*in-fiber out-of-band*) or on a separated IP network (*out-of-fiber*). Moreover, control and data information in GMPLS do not have to

¹The implementation of management communications network remains out of the scope of this paper and will not be analyzed here.

be congruently routed. This opens the possibility of deploying *asymmetrical* control plane topologies, instead of the usual *symmetrical* topologies [10] in the *in-band* configurations.

This separation between control and data planes provides several benefits to the network operators, such as an enhanced flexibility in the control deployment or the possibility to run control-plane-driven data plane recovery mechanisms (e.g., [11]–[14]), especially in the *out-of-fiber* configuration, where the control plane remains alive upon data plane failures. However, it also poses the new challenges of designing the control plane efficiently, as well as providing it with resilience to fulfill the necessities of emerging services.

Looking at the literature, some works have addressed the resilience of the GMPLS-enabled control plane. Amongst them, [9] and [10] highlighted the reasons of a decoupled control plane in all-optical networks and addressed the resilience requirements that this would impose. In addition, [15] and [16] concluded that the most severe GMPLS protocol disruptions due to message losses were found in RSVP-TE. In particular, the authors in [16] introduced a new parameter (P_d) to quantify the resilience of the GMPLS control plane. The analytical formulation in that work was only valid for *symmetrical* ring control planes, notwithstanding. More recently, this formulation has been extended to *asymmetrical* meshed control planes in [17].

In next-generation optical networks, every control plane link counts for two full-duplex control interfaces (e.g., two light transmitter-receiver pairs in the *in-fiber* control plane configuration) that must be equipped, configured, and managed, thus increasing both Capital Expenditures (CAPEX) and Operational Expenditures (OPEX). Hence, significant cost savings can be expected from reducing the number of control plane links. Notice, however, that a reduction of control plane links increases the amount of control information in the remaining ones, which accentuates the negative effects of control plane link failures. Moreover, the resulting control plane paths become also longer, and so the data plane failure recovery times if control-plane-driven restoration is implemented in the network. To the best of our knowledge, no work has still covered an independent GMPLS control plane design regardless of the data plane, which, as mentioned above, becomes crucial to leverage CAPEX and OPEX reduction in optical networks.

This paper proposes different methods for designing an optimal GMPLS control plane topology subject to specific resilience requirements. Such requirements are given in terms of P_d and Δt , based on the contributions in [16] and [17]. In particular, P_d represents the probability that any connection setup or teardown is dropped due to a control plane link failure. In turn, Δt stands for the control plane link failure recovery time, a value given by the control plane recovery mechanism implemented in the network. Then, P_d arises as a measure of the deployed control plane topology, giving insight into the transient network Grade of Service (GoS) degradation during Δt . In this work, we do not consider any influence of the control plane P_d on the average network blocking probability (P_b) as, in practical network situations, Δt will always be much lower than the network mean time to failure.

The remainder of this paper continues as follows. Section 2 reviews basic background on control plane resilience and its quantification. Section 3 introduces the problem of finding an

optimal control plane topology subject to certain resilience requirements as a non-linear combinatorial model. Being the scalability of the combinatorial model quite poor, Section 4 reformulates the problem as an iterative method that solves a constructive linear model. This method is subsequently evaluated over three alternative reference network topologies in Section 5. Finally, Section 6 concludes the paper.

II. BACKGROUND IN CONTROL PLANE RESILIENCE QUANTIFICATION

This section provides initial background on control plane resilience quantification. The concepts presented in this section will be used in the remainder of the paper.

As defined in the previous section, P_d is the probability that any connection request or teardown message becomes affected by a control plane link failure during the failure recovery time Δt (i.e., it is forwarded onto the failed link). Equation (1) reproduces the analytical P_d expression obtained in [16], which depends on the incoming (Poisson) traffic characteristics (λ, μ), Δt and P_L , being the latter the probability that an incoming connection setup/teardown is supported on the failed control plane link. In this expression, C identifies the number of active connections in the network at the failure time, that is, $C = \text{ceil}(\lambda(1 - P_b)/\mu)$, which can be approximated as $C \approx \text{ceil}(\lambda/\mu)$. This assumption holds even for significant load and P_b values ($\sim 1\%$), showing low relative errors over (1)

$$\begin{aligned} P_d &= 1 - e^{-\lambda\Delta t(1+P_L)} \cdot \sum_{k=0}^C \binom{C}{k} [(e^{\mu\Delta t} - 1) \cdot (1 - P_L)]^k \\ &= 1 - e^{-\lambda\Delta t(1+P_L)} \cdot [1 + (e^{\mu\Delta t} - 1) \cdot (1 - P_L)]^C \quad (1) \end{aligned}$$

Note that the mathematical analysis behind P_d is valid to any network scenario, as it depends mostly on the traffic characteristics. In fact, the only parameter that captures the network topology under study and the distribution of the traffic demands over it is P_L .

Let $G_{DP}(N_{DP}, E_{DP})$ and $G_{CP}(N_{CP}, E_{CP})$ identify the data and control plane graphs of a GMPLS-enabled transport network, respectively, where N_{DP} and N_{CP} represent the sets of nodes and E_{DP} and E_{CP} the sets of arcs. For the ongoing model, we assume that G_{DP} is two-connected and planar. Moreover, we also assume that G_{CP} is two-connected (e.g., a Hamiltonian cycle or a minimum n-tree), providing survivability to the control plane. Particularly, we restrict the control plane topology to be a subset (or the complete set) of the data plane one. Thus, G_{DP} and G_{CP} can be related as

$$N_{CP} \equiv N_{DP} \equiv N \quad (2)$$

$$E_{CP} \subseteq E_{DP}. \quad (3)$$

Under these assumptions, we define a minimal two-connected covering topology on G_{DP} , where E_{DP}^{it} identifies the subset of links composing this minimal topology and E_{DP}^{ot} the subset containing the rest of data plane links. Hence, $E_{DP} = E_{DP}^{it} \cup E_{DP}^{ot}$. In what follows, the additional relation between G_{DP} and G_{CP} is imposed

$$E_{CP} \supseteq E_{DP}^{it}. \quad (4)$$

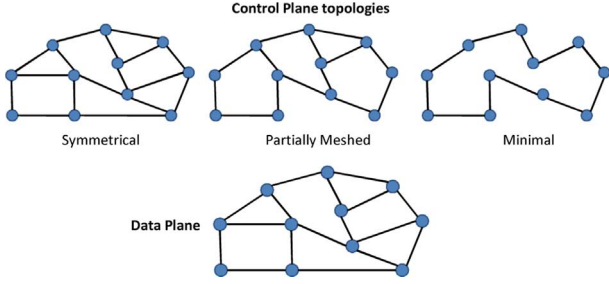


Fig. 1. Data plane topology (bottom) and three different two-connected control plane topologies: *symmetrical* (left), *partially-meshed* (center), and *minimal* (right).

The *minimal* control plane topology is defined as $E_{CP} = E_{DP}^{it}$. On this basis, any intermediate topology (hereafter, *partially-meshed*) is created by adding links to the *minimal* topology, finally reaching the *symmetrical* one ($E_{CP} = E_{DP}$). From the assumptions above, note that G_{CP} describes one ring at least (Fig. 1).

Independently from the traffic characteristics, we define D_T as the set of end-to-end demands in the network. Since G_{DP} and G_{CP} can represent different topologies, we differentiate the set of demands supported on a certain control plane link i (D_i^{CP}) from those supported on a given data plane link j (D_j^{DP}). Let us also define $\langle H_{DP} \rangle$ and $\langle H_{CP} \rangle$ as the average hop length of the data and control plane paths, respectively. As RSVP-TE messages forwarded on the control plane should visit (i.e., configure) the same node sequence comprised in the computed data plane route, $\langle H_{CP} \rangle$ becomes a function of G_{DP} and G_{CP} .

At this point, we can introduce P_L as the mean number of demands supported on a control plane link divided by the total number of demands. From another point of view, P_L can be also expressed as a function of the average control plane path length. Equation (5) expresses these alternative P_L definitions

$$P_L = \frac{\sum_{\forall i \in E_{CP}} |D_i^{CP}|}{|E_{CP}|} \cdot \frac{1}{|D_T|} = \frac{\langle H_{CP} \rangle}{|E_{CP}|}. \quad (5)$$

Obviously, a fixed number of control plane links can define several control plane topologies. Each of these topologies can lead to a different P_L value and, consequently, a different P_d .

To exemplify this, we have taken the data plane topology in Fig. 1, where we have assumed that $\lambda = 0.075 \text{ s}^{-1}$, $\mu = 0.01 \text{ s}^{-1}$ and $\Delta t = 1.5 \text{ s}$. In this scenario, we have also set the number of control plane links to 14 (as in the *partially-meshed* topology depicted in the same figure). Then, by simulation, we have calculated the maximum and minimum P_d values amongst all different control plane topologies that can be built over the data plane. From the obtained results, we have found that P_d ranges from 3.5% in the optimal control plane topology to 5.75% in the weakest one. Hence, a given number of control plane links do not necessarily assure optimal control plane resilience. In fact, their correct placement becomes essential to provide cost-effective and survivable control planes. This issue arises as an additional motivation to our work. Starting to address it, the ARCO problem is introduced in the following section.

III. RESILIENCE-AWARE GMPLS CONTROL PLANE NETWORK OPTIMIZATION PROBLEM (ARCO)

In this section, we introduce the problem of designing, for a given data plane topology, the optimal control plane topology that fits the requested resilience requirements (quantified by a requested P_d and Δt values). Besides, this service condition must be guaranteed for a given range of traffic intensities. We refer to this problem as ARCO throughout the paper.

For the definition of ARCO, we initially present a non-linear combinatorial model that chooses the optimal control plane topology from $\Gamma(G_{DP})$, that is, the set of pre-computed candidate control plane topologies over G_{DP} . Every candidate topology must follow (2)–(4), so that the *minimal*, the *symmetrical* and a large number of *partially-meshed* topologies are included in $\Gamma(G_{DP})$. Then, for each control plane topology g in $\Gamma(G_{DP})$, we compute P_L^g and its cost A^g (i.e., the number of arcs).

The combinatorial model for the ARCO problem (ARCO-CNL) uses the following sets and parameters:

G_{DP}	Data plane graph
$\Gamma(G_{DP})$	Set of candidate control plane topologies built over the data plane topology G_{DP} , index g
A^g	Cost of the candidate topology g
P_L^g	P_L of the candidate topology g
Λ	Set of arrival rates
μ	Average service rate
Δt	Failure recovery time
P_d^{\max}	Maximum allowed P_d

Additionally, the variable γ^g is defined, which equals 1 if and only if the control plane topology g is optimal. Using this notation, we can formulate ARCO-CNL as

$$\text{(ARCO-CNL) Minimize } |E_{CP}| = \sum_{\forall g \in \Gamma(G_{DP})} A^g \cdot \gamma^g \quad (6)$$

subject to :

$$\sum_{\forall g \in \Gamma(G_{DP})} \gamma^g = 1 \quad (7)$$

$$P_d(\lambda_i, \mu, \Delta t, P_L^g) \cdot \gamma^g \leq P_d^{\max} \quad \forall g \in \Gamma(G_{DP}), \lambda_i \in \Lambda \quad (8)$$

$$\gamma^g \in \{0, 1\}, \quad \forall g \in \Gamma(G_{DP}). \quad (9)$$

Constraint (7) ensures that only one control plane topology is chosen. Constraint (8) guarantees that P_d^g is lower than P_d^{\max} for all the traffic intensities under consideration. Finally, constraint (9) defines γ^g as binary.

The number of variables and constraints in ARCO-CNL is proportional to the summation of the number of $|E_{DP}^{ot}|$ -element subsets of an $(|E_{DP}| - |E_{DP}^{it}|)$ -element set, from the *minimal* to the *symmetrical* topology. Thus

$$\begin{aligned} |\Gamma(G_{DP})| &\approx \sum_{|E_{DP}^{ot}|=0}^{|E_{DP}| - |E_{DP}^{it}|} \binom{|E_{DP}| - |E_{DP}^{it}|}{|E_{DP}^{ot}|} \\ &= 2^{|E_{DP}| - |E_{DP}^{it}|}. \end{aligned} \quad (10)$$

TABLE I
PRE-PROCESSING ALGORITHM FOR ARCO-CNL

<p>Input: G_{DP}, D_T Output: set $\Gamma(G_{DP})$, set P_L, set A.</p> <p>Initialize $\Gamma(G_{DP}) = \emptyset$ Initialize $P_L = \emptyset$ Initialize $A = \emptyset$</p> <p>while more candidate control plane topologies can be found do Find new control plane topology g A^g=number of links of topology g Compute $\langle H_{CP} \rangle$ of traffic demand D_T over topology g $P_L^g = \langle H_{CP} \rangle / A^g$ Update sets $\Gamma(G_{DP}), A, P_L$</p>

Considering that the whole $\Gamma(G_{DP})$ set has to be explored to find the optimal solution, the ARCO-CNL problem can be classified as NP-Complete. Furthermore, its formulation requires a pre-computation of the set of candidate topologies, as well as the calculation of their respective P_L^g and A^g values.

Table I shows a procedure to obtain this input data for ARCO-CNL. The complexity of a single iteration in this pre-processing algorithm is given by the complexity to compute all shortest paths between each pair of adjacent nodes in the data plane over the candidate control plane topology g . This can be approximated to $|E_{DP}|$ times the complexity of the Dijkstra shortest-path algorithm that, from [18], equals $O(|E_{DP}| * \log|N|)$. Hence, the resulting pre-processing algorithm complexity raises to $O(|E_{DP}|^2 * \log|N| * 2^{|E_{DP}| - |N|})$.

Note that the complexity of the proposed combinatorial model (i.e., pre-processing plus mathematical programming) clearly leads to unacceptable solving times. Indeed, this model was only intended to be an initial formulation of ARCO. In the following section, we present an improved constructive method that builds itself feasible topologies from a pre-computed set of routes given G_{DP} .

IV. ARCO CONSTRUCTIVE METHOD

As mentioned in Section II, the RSVP-TE protocol messages are processed hop-by-hop in every node composing the route of the connection to be setup or torn-down. From (3), adjacent nodes in the data plane may be not adjacent in the control plane. As a result, $\langle H_{CP} \rangle$ is proportional to $\langle H_{DP} \rangle$. Then, P_L can be re-written as

$$P_L = \frac{\tau \cdot \langle H_{DP} \rangle}{|E_{CP}|}. \quad (11)$$

Here, the parameter τ adjusts the distance in the control plane between those adjacent nodes in the data plane (i.e., the number of hops). In other words, τ represents the average number of control plane hops between a pair of data plane adjacent nodes. To evaluate τ , we consider the number of hops in the control

plane (h_i^{CP}) for a given data plane link, weighted by the number of demands supported on this link

$$\tau = \frac{\sum_{i \in E_{DP}} h_i^{CP} \cdot |D_i^{DP}|}{\sum_{i \in E_{DP}} |D_i^{DP}|}. \quad (12)$$

Note that P_L depends on the traffic distribution, as it is proportional to $\langle H_{DP} \rangle$. In this work, we assume a uniform traffic distribution. In such a case, having enough data plane resources (e.g., wavelengths), every demand is routed through its shortest path. Hence, $\langle H_{DP} \rangle$ (and also P_L) can be computed irrespective of the offered load. Proposition 1 relates P_d values for different traffic intensities.

Proposition 1: Given a set of constant (and strictly positive) parameters ($\mu, \Delta t$, and P_L) and two arrival rates λ_1 and λ_2 , it is accomplished that

$$P_d^1(\lambda_1, \mu, \Delta t, P_L) > P_d^2(\lambda_2, \mu, \Delta t, P_L) \quad \forall \lambda_1 > \lambda_2. \quad (13)$$

Proof: The partial derivate of P_d with respect to λ (14) is strictly positive

$$\frac{\partial P_d}{\partial \lambda} = f(\mu, \Delta t, P_L) \cdot e^{-\lambda \Delta t (1 + P_L)} > 0. \quad (14)$$

Here, f is a strictly positive function that depends only on $\mu, \Delta t$, and P_L . As the exponential function is an increasing continuous function, the partial derivate is positive in the whole λ domain. Therefore, P_d is continuous and increasing with λ . \square

Proposition 1, jointly with the assumption of independence between P_L and the traffic parameters, allows us to obtain the optimal control plane topology by solving the ARCO-CNL problem only for the highest traffic intensity. In order to reduce the number of variables in our problem even more, we also define a constructive method for ARCO, different than the combinatorial approach proposed in Section III.

With such purposes in mind, we could have introduced a model that minimizes the number of control plane links. Then, a constraint ensuring $P_d \leq P_d^{\max}$ would have had to be included, turning the model into non-linear. This would have prevented the use of efficient linear solvers, raising the ARCO execution times eventually. In contrast, a linear ARCO model is attempted in this section. We denote it as ARCO-IL. In order to define this model, the following mathematical propositions that relate P_d, P_L and E_{CP} have to be introduced.

Proposition 2: Given a set of constant parameters (λ, μ , and Δt) and two different values of P_L (P_L^1 and P_L^2), all strictly positive, it is accomplished that

$$P_d^1(\lambda, \mu, \Delta t, P_L^1) < P_d^2(\lambda, \mu, \Delta t, P_L^2) \quad \forall P_L^1 < P_L^2. \quad (15)$$

Proof: Using the same argument as in Proposition 1, the partial derivate of P_d with respect to P_L is

$$\frac{\partial P_d}{\partial P_L} = (1 - P_d) \left(\lambda \Delta t + C \cdot \frac{e^{\mu \Delta t} - 1}{1 + (e^{\mu \Delta t} - 1) \cdot (1 - P_L)} \right). \quad (16)$$

Since P_L is a value comprised between (0, 1], and the other parameters are strictly positive, the derivate is strictly positive unless P_d equals 1. This happens when the connection inter-arrival time is lower than the control failure recovery time (i.e., $\lambda * \Delta t > 1$), which is far from the usual traffic dynamics in circuit-switched networks. As will be discussed in Section V, few seconds can be expected to recover the control plane in GMPLS-controlled transport networks. These times are much lower values than the expected minutes or hours' inter-arrival times to make circuit-switching efficient. Therefore, we can consider $P_d < 1$ in all cases, being an increasing continuous function with respect to P_L . \square

Proposition 2 allows to ensure that a control plane topology minimizing P_d for a given set of feasible control plane topologies and a set of traffic parameters also minimizes P_L .

Proposition 3: Let G_{CP}^1 and G_{CP}^2 be two different control plane topologies over the same data plane topology G_{DP} that satisfy

$$|E_{CP}^1| > |E_{CP}^2|. \quad (17)$$

Furthermore, let P_L^1 and P_L^2 be the P_L values for these topologies, respectively. If both G_{CP}^1 and G_{CP}^2 are optimal graphs with respect to P_d , it is accomplished that

$$P_L^1 < P_L^2. \quad (18)$$

Proof: From (12) and (17), the summation of h_i^{CP} is lower in G_{CP}^1 than in G_{CP}^2 , since both are optimal graphs with respect to P_d . Then, since $\tau^1 < \tau^2$, we have that

$$P_L^1 = \frac{\tau^1 \cdot \langle H_{DP} \rangle}{|E_{CP}^1|} < \frac{\tau^2 \cdot \langle H_{DP} \rangle}{|E_{CP}^2|} = P_L^2. \quad (19)$$

\square

From Proposition 3, we can conclude that the removal of one arc from the control plane topology results in a new control plane topology with higher P_L . In addition, we can state that given $|E_{CP}|$, we can minimize P_L by minimizing τ alternatively.

With Propositions 2 and 3 in hand, we are finally able to propose ARCO-IL. Using integer linear programming, this model minimizes P_L by minimizing τ , instead of minimizing P_d directly. The integer linear model generates the optimal control plane topology with respect to P_L for a given $|E_{CP}|$. The value of P_d is computed based on the obtained P_L , ensuring that it is lower than the threshold value. This must be repeated iteratively, modifying $|E_{CP}|$.

For the ongoing formulation, a set of routes over the *symmetrical* topology are pre-computed for every data plane link. Next, a subset of these routes is chosen to provide control plane connectivity to every data plane link. Finally, a subset of E_{DP} is added to E_{CP} to make these routes feasible.

In addition to the notation previously defined, the following sets and parameters are used for ARCO-IL:

E_{DP}	Set of links in the data plane
E_{CP}	Set of links in the control plane

$R(i)$	Set of control plane routes for data plane link i . A control plane route is a path between the end nodes of a data plane link over the <i>symmetrical</i> topology.
Q_{ijk}	Equal to 1 if the control plane route j for data plane link i uses control plane link k , 0 otherwise
C_{ij}	Cost (in number of hops) of control plane route j for data plane link i .
D_i^{DP}	Set of connections supported on data plane link i
D_T	Set of connections offered to the network
ρ	Predefined number of control plane links
M	A large positive constant

Additionally, the following variables are used:

ζ_k	Equal to 1 if link k is created in the control plane, 0 otherwise.
ω_{ij}	Primary route. Equal to 1 if data plane link i is assigned to the control plane route j , 0 otherwise.
κ_{ij}	Back up route. Equal to 1 if data plane link i is assigned to the control plane route j , 0 otherwise.

Using this notation, we can redefine the parameter τ as

$$\tau = \frac{\sum_{\forall i \in E_{DP}} (|D_i^{DP}| \cdot \sum_{\forall j \in R(i)} (C_{ij} \cdot \omega_{ij}))}{\sum_{\forall i \in E_{DP}} |D_i^{DP}|}. \quad (20)$$

As a result, the integer linear programming model for ARCO-IL becomes

$$\text{(ARCO-IL) Minimize } \tau \quad (21)$$

subject to

$$\sum_{\forall j \in R(i)} \omega_{ij} = 1 \quad \forall i \in E_{DP} \quad (22)$$

$$\sum_{\forall j \in R(i)} \kappa_{ij} = 1 \quad \forall i \in E_{DP} \quad (23)$$

$$\sum_{\forall j \in R(i)} Q_{ijk} \cdot (\omega_{ij} + \kappa_{ij}) \leq 1 \quad \forall i, k \in E_{DP} \quad (24)$$

$$\left(\sum_{\forall k \in E_{DP}} \zeta_k \cdot Q_{ijk} \right) - C_{ij} + M \cdot (1 - \omega_{ij} - \kappa_{ij}) \geq 0 \quad \forall i \in E_{DP}, j \in R(i) \quad (25)$$

$$\sum_{\forall k \in E_{DP}} \zeta_k = \rho \quad (26)$$

$$\zeta_k, \omega_{ij}, \kappa_{ij} \in \{0, 1\} \quad \forall i, k \in E_{DP}, j \in R(i). \quad (27)$$

Fixing the number of control plane links and based on (11), the objective function (21) minimizes τ using the definition provided in (20).

Constraints (22), (23) and (24) ensure the two-connectivity at control plane. Constraint (22) guarantees that every data plane link has one primary control plane route, whereas constraint (23) guarantees one back up route. Constraint (24) ensures that both control plane routes are link-disjoint. Constraint (25) makes sure that all control plane routes only use active control plane links.

TABLE II
ARCO-IL METHOD

<p>Input: G_{DP}, D_T, set Λ, μ, Δt, P_d^{max} Output: G_{CP}.</p> <p>Let ρ as the fixed number of control plane links</p> <p>Compute $\langle H_{DP} \rangle$ of traffic demand D_T over the G_{DP} topology</p> <p>for every link i in E_{DP} do Compute D_i from D_T $R(i)$ = compute all routes between link i end nodes in G_{DP}</p> <p>Compute Q and C from R</p> <p>$\lambda := \max(\Lambda)$</p> <p>Set initial point for $\rho := \rho^{ini}$ Set $\rho_{ant} := \rho$</p> <p>While no Optimal G_{CP} founded do Solve ARCO-IL ILP model Evaluate P_d of obtained solution if $P_d \leq P_d^{max}$ and $\rho_{ant} < \rho$ then Optimal G_{CP} founded else if $P_d \leq P_d^{max}$ and $\rho_{ant} \geq \rho$ then Actualize incumbent G_{CP} $\rho_{ant} := \rho$ $\rho := \rho - 1$ if $\rho < E_{DP}^{it}$ then break else if $P_d > P_d^{max}$ and $\rho_{ant} > \rho$ then Optimal G_{CP} founded else if $P_d > P_d^{max}$ and $\rho_{ant} \leq \rho$ then Actualize incumbent G_{CP} $\rho_{ant} := \rho$ $\rho := \rho + 1$ if $\rho > E_{DP}$ then break</p> <p>Return G_{CP}</p>
--

Note that no additional constraint to ensure that every primary control plane route is the shortest possible one is necessary, as the length of the route is already minimized in the objective function. This allows reducing the size of the problem eventually. Constraint (26) ensures that the number of control plane links is equal to the specified number. Finally, constraint (27) defines the variables as binary.

After each ARCO-IL execution, the resulting P_d value in the obtained control plane topology is calculated using the formula in (1). Depending on the relation between this result and the maximum P_d permitted, a new iteration can be executed by modifying the number of control plane links. The algorithm ends either when the optimal solution is found or the *minimal* or the *symmetrical* topology is reached.

Table II shows the details of the ARCO-IL method. The number of iterations needed to find the optimal solution strongly depends on the *quality* of the number of control plane links initially provided. As introduced in [17], (1) allows to estimate P_d in a certain network, given a set of traffic parameters and the characteristics (nodes and arcs) of both control and data planes. Departing from this expression and using statistical inference techniques over the observed values, we have obtained a two-step procedure to predict the number of control plane links from P_d and a certain set of traffic and data plane characteristics.

Firstly, we have approximated the inverse of (1) as follows, which allows us obtaining P_L from P_d

$$P_L \cong \left(\frac{1}{2 \cdot \lambda \cdot \Delta t \cdot |N|} + \frac{1}{10} \right) \cdot P_d. \quad (28)$$

Secondly, we have obtained an expression to estimate the number of links in the control plane given the objective P_L value and the number of nodes and links in the data plane. We denote δ_{DP} to the average nodal degree in the data plane

$$\rho^{ini} = \left\lceil \left(\frac{5}{4} \cdot |E_{DP}| \right) \cdot (1 - P_L) \left[\left(\frac{|N|}{25} + 2 \right) \cdot \delta_{DP} + \frac{|N|}{5} \right] + |N| \right\rceil. \quad (29)$$

The obtained ρ^{ini} value estimates the number of links in the optimal control plane topology and can be used as the initial point for the ARCO-IL method.

The complexity of the ARCO-IL pre-computing algorithm can be derived from the complexity to obtain all routes in the control plane for each pair of data plane adjacent nodes. Let us define $Rmax$ as the maximum number of feasible control plane routes between a pair of data plane adjacent nodes. Then, the algorithm's complexity becomes $O(Rmax * |E_{DP}| * \log |N|)$. As can be seen, the number of control plane routes influences the size and the execution time of ARCO-IL. Note that all control plane routes for each pair of data plane adjacent nodes need to be computed to ensure two-connectivity of the control plane.

Analyzing the size of the ARCO-IL model, the number of variables and constraints can be approximated by $2 * |E_{DP}| * Rmax$ and $|E_{DP}| * (|E_{DP}| + Rmax)$, respectively. Then, as the ARCO constructive method is iterative, its total execution time is given by K times the solving time of one integer linear model. Note that the worst performance appears when ρ^{ini} is the maximum number of control plane links (i.e., $|E_{DP}|$), but the optimal topology requests the minimum number of links (i.e., $|E_{DP}^{it}|$). In this case, $|E_{DP}| - |E_{DP}^{it}|$ iterations are required. Contrarily, the best performance is achieved if ρ^{ini} equals the number of control plane links in the optimal topology. In this case, only two iterations are needed, namely, a first one to obtain the optimal topology and a second one to verify the optimality. Being the optimal solution coincident with the *symmetrical* or the *minimal* topology, the final optimality verification might not be needed if ρ^{ini} predicts it. In the following section, we evaluate the average number of ARCO-IL iterations in different networks, validating the performance of the proposed method as well as the accuracy of ρ^{ini} .

V. ILLUSTRATIVE NUMERICAL RESULTS

The performance of the proposed ARCO methods has been validated over three network topologies with different average node degree. More precisely, we have considered a quite sparse 28-Node NSFNET topology and two moderately meshed topologies: the 14-Node Deutsche Telekom (DT) network, and a large 37-Node European Optical Network (EON). Fig. 2 shows the topologies under consideration and reviews their most relevant characteristics.

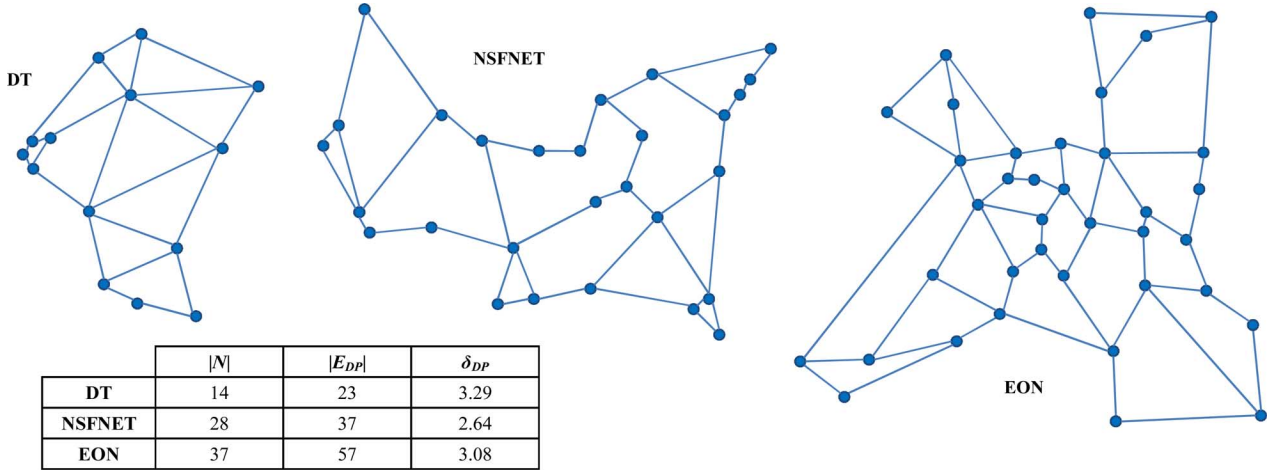


Fig. 2. Sample transport network topologies used in this paper: 14-Node Deutsche Telekom (DT) (left), 28-node NSFNET (center), and 37-Node European Optical Network (right). A table with their most relevant characteristics is also provided.

TABLE III
SIZE OF ARCO-CNL AND ARCO-IL METHODS

	ARCO-CNL		ARCO-IL		
	Vars.	Cons.	Vars.	Cons.	$\Sigma R(i)$
DT	2^9	$2^9 \Lambda $	2,503	1,816	1,240
NSFNET	2^8	$2^8 \Lambda $	3,675	3,263	1,819
EON	2^{18}	$2^{18} \Lambda $	591,151	298,911	295,547

Table III shows the complexity of ARCO-CNL and ARCO-IL in terms of the mathematical programming problem size. As seen, the number of topologies in ARCO-CNL grows exponentially, as predicted in (10). Due to the size of the mathematical programming problem and the complexity of the pre-processing algorithm, ARCO-CNL leads to intractable problems, even for relatively small instances. Furthermore, its non-linear nature increases its overall complexity even more.

Even though the dimensions of ARCO-CNL and ARCO-IL are not strictly related, the number of constraints can be reduced by a $|\Lambda|$ factor (the number of traffic intensities), as a consequence of Proposition 1. The size of an ARCO-IL instance directly depends on the characteristics of the network topology under evaluation. While the size becomes small and similar for both DT and NSFNET networks, it is a hundred times larger for the EON, which is translated into more complex instances and slower convergence times. Recall that ARCO-IL needs to pre-compute the set of control plane routes for every data plane link ($R(i)$). The total number of pre-computed routes is presented in the last column of Table III, which increase in a similar way as the number of variables and constraints in the different topologies.

Concerning the number of iterations in ARCO-IL, we discussed that it depends on the quality of the initial point (ρ^{ini}). Interestingly, we found that ARCO-IL did not require more than three iterations in any experiment conducted on the DT, NSFNET or EON networks, proving the high precision of the expressions in (28) and (29).

Additionally, the performance and accuracy of the model have been validated by simulation. For these experiments, 32

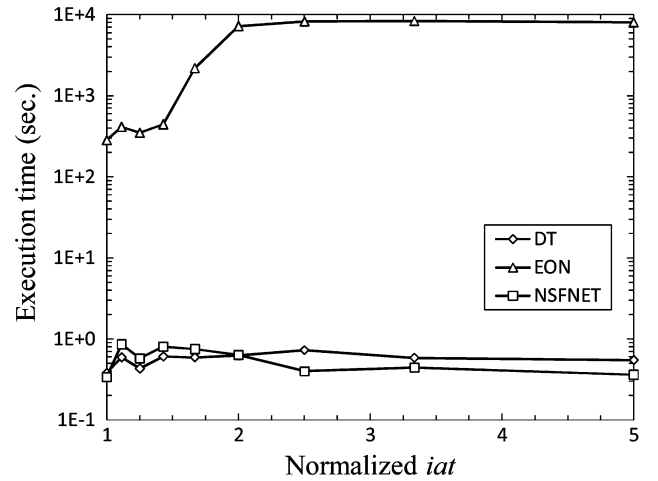


Fig. 3. ARCO-IL execution time for the EON, DT and NSFNET topologies as a function of the inter-arrival time.

bidirectional wavelengths per link have been considered in all network topologies, where uniformly distributed connection requests arrive at each node following a Poisson process. Moreover, exponentially distributed connection holding times ($ht = 1/\mu$) have been also assumed.

As obtained in [16], P_d depends highly on the connection inter-arrival time ($iat = 1/\lambda$) rather than on the connection holding time ($ht = 1/\mu$) for a given offered load. Taking this into account, in the experiments that follow we set the maximum offered load that can be offered to the network without violating the $P_b < 1\%$ requirement. In such a high load scenario, we quantify the benefits of using ARCO-IL for different iat (and consequently ht) values. Note, however, that the λ/μ quotient (i.e., the offered load) is kept constant in the graphs. Besides, for better illustration, the inter-arrival times in the considered scenarios have been normalized to the value such that the optimal control plane topology is equal to the *symmetrical* topology under the most stringent resilience requirements.

In particular, we have considered two alternative sets of control plane resilience requirements, namely, $RRq1$ and $RRq2$,

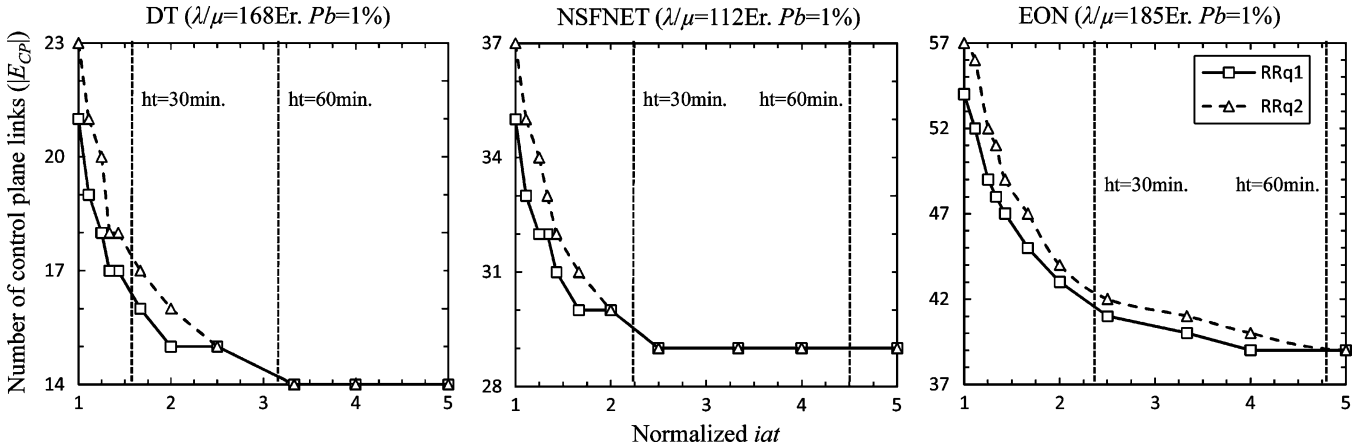


Fig. 4. Number of links in the optimal control plane solution as a function of the iat for DT (left), NSFNET (center), and EON (right). The offered load have been fixed so that $P_b = 1\%$.

which would illustrate two different network situations. *RRq1* identifies the situation where $P_d \leq 5\%$ must be assured having a recovery mechanism able to restore the control plane in $\Delta t \leq 1.5$ s. Alternatively, *RRq2* depicts a different scenario where $P_d \leq 10\%$ must be satisfied, but having a slower control plane recovery mechanism able to restore a control plane failure in $\Delta t \leq 3.5$ s.

Without going into the details of the recovery mechanisms, the $\Delta t \leq 1.5$ s in *RRq1* could be achieved with control plane link failure detection based on LMP (failure detection time < 450 ms [8]) and pre-computed backup control channels (e.g., using hop-by-hop explicit IP routing or MPLS tunneling). For the $\Delta t \leq 3.5$ s in *RRq2*, LMP-based control plane link failure detection and standard IP layer re-routing might be enough. Here we would assume that the IP forwarding in the network can converge dynamically in approximately 3s from the failure detection.

The ARCO-IL method was implemented in iLog-OPL and solved by the CPLEX v.11.0 optimizer [19] on a 2.4 GHz Quad-Core machine with 8 GB RAM memory. Fig. 3 shows the obtained execution times for ARCO-IL as a function of the inter-arrival time to the test topologies.

From the obtained results, the execution times are in line with the size of the ARCO-IL instances. As seen, sub-second execution times are achieved in the DT and NSFNET topologies, whereas tens of minutes to several hours are required in the EON. Specifically, large execution time differences are observed in the EON between short and long inter-arrival times, where the feasible solutions are relatively reduced or numerous, respectively.

Fig. 4 shows the number of links in the optimal control plane topology as a function of the normalized iat in the DT, NSFNET, and EON topologies. Note that the y-axis of the graphs comprises the number of control plane links from the *minimal* to the *symmetrical* topology in each case. Moreover, each graph contains two separated plots, one for *RRq1* and another for *RRq2*. Looking at the results, the optimal control plane topology tends to be the *symmetrical* one for short inter-arrival times. Conversely, when the iat increases, the number of control plane links decreases, finally reaching the *minimal* topology.

TABLE IV
RESTORATION TIMES

	Symmetrical	Partially meshed	Minimal
DT	35.33 ms	39.27 ms	40.32 ms
NSFNET	78.31 ms	94.39 ms	102.96 ms
EON	64.25 ms	75.74 ms	93.26 ms

Aiming to evaluate the actual cost reduction achieved by means of ARCO-IL, we have highlighted in Fig. 4 two particular ht values, $ht = 30$ min and $ht = 60$ min. As shown, the minimal control plane topology could be almost reached in the DT, NSFNET and EON networks for $ht = 60$ mins. This enables a reduction of 8, 8, and 18 control plane links, respectively. For $ht = 30$ min, since the connection iat is reduced, a quite lower reduction is achieved, enabling 6, 7 and 15 control plane links to be removed from the *symmetrical* topology for the most stringent requirements, respectively. Note that such savings are obtained in practical core network scenarios under high traffic loads, which makes them especially interesting.

As mentioned in the introduction, link reduction in the control plane may affect connection establishment and restoration times, since signaling messages must travel longer distances. In order to better assess the outcome of ARCO-IL, we have quantified such increments using the equation proposed in [20] for intra-domain restoration, which has been adapted to fit single domain scenarios. The obtained results in the DT, NSFNET and EON networks are depicted in Table IV, where the optimal partially-meshed topology resulting from ARCO-IL for $ht = 30$ min is compared to the *symmetrical* and *minimal* topologies. As seen, the *symmetrical* topology provides the minimum restoration times as no link reduction is done. Average restoration times under 50 ms can be obtained only for the DT network as a consequence of the shorter link lengths; in contrast longer restoration times can be expected for the NSFNET and EON networks. The restoration times achieved in the partially-meshed topology, and even in the *minimal* topology, are still very reasonable, around 100 ms in the worst case. Note that restoration times under 50 ms can be still obtained for the DT network over the *minimal* topology.

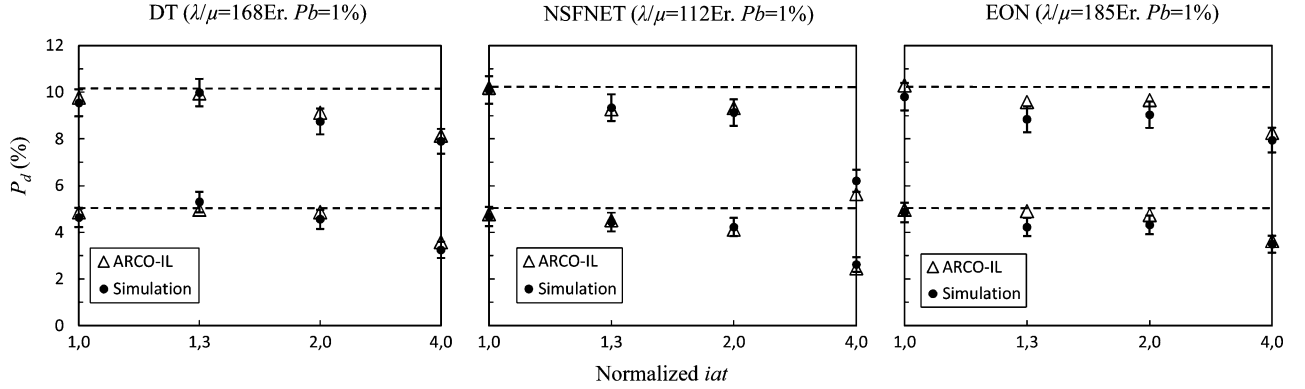


Fig. 5. P_d as a function of the iat for the different network topologies: DT (left), NSFNET (center), and EON (right). Lower series are for $RRq1$ whereas upper ones are for $RRq2$.

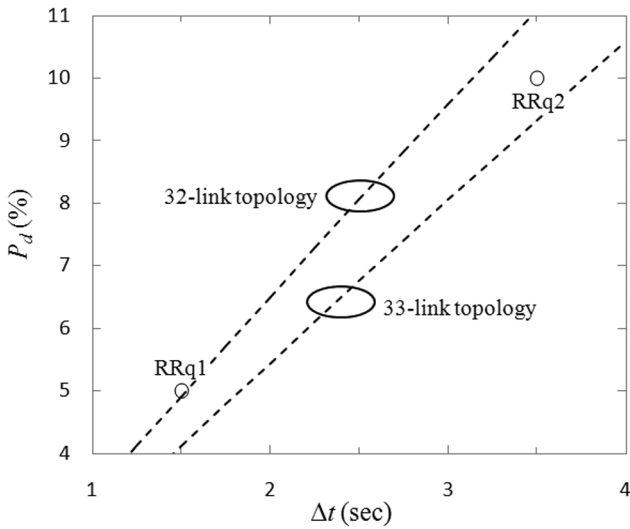


Fig. 6. P_d against Δt for two control plane networks over the NSFNET topology. The 32-link topology satisfies $RRq1$ but not $RRq2$. The 33-link topology satisfies both $RRq1$ and $RRq2$.

Fig. 5 compares the expected P_d values by ARCO-IL to the ones obtained by simulation in the DT, NSFNET and EON networks for four different normalized iat values. Each graph contains two plots, one for each set of resilience requirements. As seen, the results validate the assumptions done and the model defined in this paper, since most of the obtained values by ARCO-IL lie within the 95% confidence interval of the simulation results. Specifically, the ARCO-IL method chooses these topologies with expected P_d value as close as possible and below the threshold value. For large iat values, the optimal solution is limited by the set of constraints over the characteristics of the feasible topologies (basically the two-connected requirement), and the *minimal* topology is chosen. On the contrary, if no optimal solution is found, ARCO-IL selects the *symmetrical* topology as the best solution, although the P_d requirement cannot be satisfied. In particular, having a P_d value significantly below the threshold, a post-processing method can be additionally applied to relax the resilience requirements, as it will be presented later.

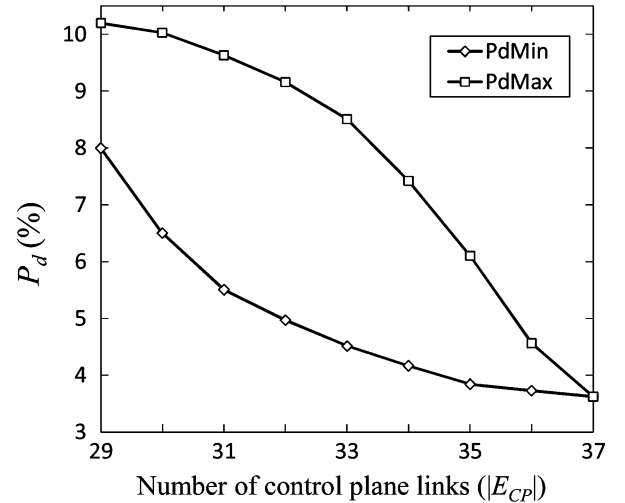


Fig. 7. Minimum and maximum P_d values as a function of the number of control plane links in the NSFNET network.

From the results in Fig. 4, a similar cost reduction is achieved no matter if $RRq1$ or $RRq2$ requirements are matched. However, extra links are needed in the optimal control plane topology to satisfy $RRq2$, even permitting a higher P_d value. Fig. 6 shows the explanation to this fact in the NSFNET topology. Remember that $RRq1$ and $RRq2$ have been defined as a tuple of P_d and Δt values. Therefore, providing the control plane recovery mechanism a specific Δt value, we can create more or less stringent requirements by modifying P_d accordingly, which finally results into different optimal control plane topologies. However, as P_d and Δt are related by (1), the final requested resilience to the network cannot be appreciated by comparing P_d and Δt independently. This has been illustrated in Fig. 6. Although $RRq1$ seems to be more restrictive than $RRq2$ when comparing the allowed P_d and Δt values independently, more links in the optimal control plane topology are needed for $RRq2$, as the overall requested resilience is higher in this case.

Fig. 7 corroborates the usefulness of ARCO-IL method to find the optimal control plane topology among a range of feasible topologies with a specific number of control plane links. These control plane topologies are obtained in the NSFNET network

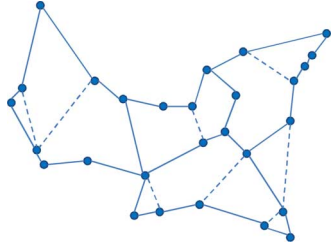


Fig. 8. An example of optimal control plane topology for NSFNET. Dotted lines represent unused links.

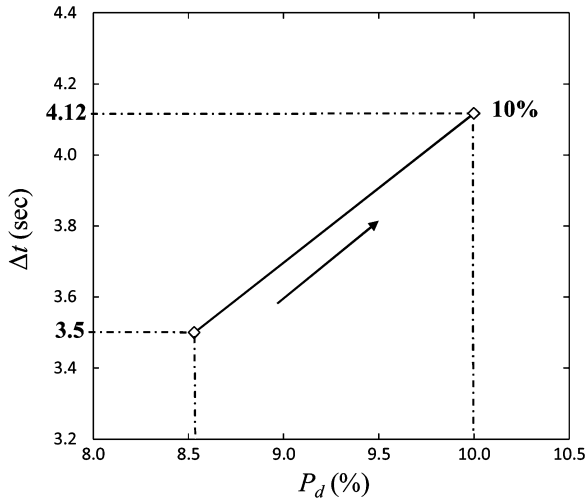


Fig. 9. Example of sensibility analysis (Δt against P_d). Control plane recovery requirements are relaxed, reducing related network costs.

under a normalized iat equal to 1.3 and $\Delta t \leq 3.5$ s. For illustration purposes, we used a slightly modified version of ARCO-IL to obtain the maximum P_d value resulting from the worst control plane topology (where τ is maximized), so that we can compare it to the optimal one afterwards. As shown, the optimal control plane topologies found by ARCO-IL allow a P_d reduction of more than 50% with respect to the worst control plane topology.

Finally, Fig. 9 addresses a sensitivity analysis of P_d against Δt in an optimal control plane topology. For this purpose, we have focused on the NSFNET topology with a normalized iat equal to 2.5. Assuming that the resilience requirements in *RRq2* have to be matched, ARCO-IL comes up with the optimal control plane topology depicted in Fig. 8, where 8 control plane links are saved compared to the *symmetrical* one. This optimal control plane topology leads to $P_d \approx 8.5\%$ for $\Delta t = 3.5$ s. Nevertheless, Δt can still be increased to 4.12 s before reaching the $P_d = 10\%$ threshold, as observed in Fig. 9. This new Δt value may allow the deployment of simpler control plane recovery mechanisms, yielding reduced network costs while still matching the required control plane resilience.

VI. CONCLUDING REMARKS

This work addressed, for the first time, the design of the control plane topology in GMPLS-enabled transport networks. To this goal, two challenges were initially posed: firstly, the minimization of network CAPEX and OPEX derived from the provisioning, configuration and maintenance of control

plane links; secondly, the fulfillment of the required control plane resilience to support future network services. Although a reduction of control plane links leads to lower network costs it increases however the amount of control information in the remaining control plane links, accentuating the negative effects of control plane link failures and leading to degraded network resilience performance. Therefore, control plane design methods that make a good trade-off between network cost and resilience are necessary.

Two models were proposed to solve the problem of obtaining the optimal GMPLS control plane topology given the data plane topology, a set of resilience requirements (quantified in terms of P_d and Δt) and the range of offered loads to the network. First of all, a non-linear combinatorial model of the problem (ARCO-CNL) was initially introduced. This model, however, offers a poor scalability as the network size grows up. Having this in mind, the problem was reformulated as a constructive linear model (ARCO-IL), providing optimal results with much lower execution times.

Into operation, ARCO-IL focuses on minimizing the average number of hops in the control plane for every data plane adjacent node pair, identified as τ . While P_d and P_L are non-linear functions, it was proved that τ becomes linear if the number of control plane links remains constant. In view of this, an iterative method was introduced in ARCO-IL, which modifies the number of control plane links per iteration. In order to provide an initial number of control plane links close to the optimal one, that is, minimizing the number of iterations of the method, a two-step procedure that computes this value as a function of the objective P_d was also proposed.

The performance of ARCO-IL was extensively assessed over three reference network topologies with different number of nodes and node degree. From the obtained results, ARCO-IL leads to sub-second execution times in the 14-Node DT and the 28-Node NSFNET topologies. In the 37-Node EON topology, however, even though the execution times increased significantly due to the huge network dimensions, they were still bearable. Aiming to quantify the actual cost savings achieved by applying ARCO-IL, the reduction in terms of control plane links in the optimal control plane topology against the *symmetrical* one was obtained for the DT, NSFNET and EON networks. From 6 to 15 control plane links can be reduced in high load scenarios ($P_b = 1\%$), while still meeting the required control plane resilience.

A side effect of reducing the number of control plane links can be an increment of the connection establishment times, which may be particularly critical if control-plane-driven restoration for data plane recovery is implemented. Nonetheless, we found that the restoration times over the optimal control plane topology were not highly increased compared to the *symmetrical* one, remaining below 100 ms in the three reference network topologies. As a final result, a sensitivity analysis was conducted on the optimal control plane topology provided by ARCO-IL to relax, if still possible, the control plane failure recovery time to be achieved by the control plane recovery mechanism without exceeding the specified resilience thresholds. In fact, more relaxed control plane recovery requirements opens the deployment of simpler and, thus, cheaper

control plane recovery mechanisms, reducing in this way the network costs even more.

Further research areas may entail the proposal of heuristic algorithms to provide near optimal solutions in shorter execution times, especially in very large network topologies such as the 37-Node EON.

REFERENCES

- [1] A. Jajszczyk, "Automatically switched optical networks: Benefits and requirements," *IEEE Commun. Mag.*, vol. 43, pp. S10–S15, Feb. 2005.
- [2] *Network Node Interface for the Synchronous Digital Hierarchy (SDH)*, ITU. Rec. G.707/Y.1322, Aug. 2003.
- [3] E. Rosen, A. Viswanathan, and R. Callon, "Multiprotocol label switching architecture," in *IETF RFC 3031*, Jan. 2001.
- [4] "ITU. Rec. G.8080/Y.1304: Architecture for the automatically switched optical network (ASON)," Nov. 2001.
- [5] E. Mannie, "Generalized multi-protocol label switching architecture," in *IETF RFC 3945*, Oct. 2004.
- [6] L. Berger, "Generalized multi-protocol label switching (GMPLS) signaling resource ReSerVation protocol-traffic engineering (RSVP-TE) extensions," in *IETF RFC 3473*, Jan. 2003.
- [7] D. Katz, K. Kompella, and D. Yeung, "Traffic engineering (TE) extensions to OSPF version 2," in *RFC 3630*, Sep. 2003.
- [8] J. Lang, "Link management protocol (LMP)," in *IETF RFC 4204*, Oct. 2005.
- [9] G. Li, J. Yates, D. Wang, and C. Kalmanek, "Control plane design for reliable optical networks," *IEEE Commun. Mag.*, vol. 40, pp. 90–96, Feb. 2002.
- [10] A. Jajszczyk and P. Rózycki, "Recovery of the control plane after failures in ASON/GMPLS networks," *IEEE Netw.*, vol. 20, pp. 4–10, Jan. 2006.
- [11] W. Grover, *Mesh-Based Survivable Transport Networks: Options and Strategies for Optical, MPLS, SONET and ATM Networking*. Englewood Cliffs, NJ: Prentice Hall, 2003.
- [12] J.-P. Vasseur, M. Pickavet, and P. Demeester, *Network Recovery—Protection and Restoration of Optical, SONET-SDH, IP and MPLS*. San Francisco, CA: Elsevier, 2004.
- [13] L. Velasco, S. Spadaro, J. Comellas, and G. Junyent, "Introducing OMS protection in GMPLS-based optical ring networks," *Comput. Netw.*, vol. 52, pp. 1975–1987, Jul. 2008.
- [14] L. Velasco, S. Spadaro, J. Comellas, and G. Junyent, "Shared-path protection with extra-traffic in ASON/GMPLS ring networks," *OSA J. Opt. Netw.*, vol. 8, pp. 130–145, Jan. 2009.
- [15] O. Komolafe and J. Sventek, "Impact of GMPLS control message loss," *J. Lightw. Technol.*, vol. 26, pp. 2029–2036, Jul. 2008.
- [16] J. Perelló, S. Spadaro, J. Comellas, and G. Junyent, "An analytical study of control plane failures impact on GMPLS ring optical networks," *IEEE Commun. Lett.*, vol. 11, pp. 695–697, Aug. 2007.
- [17] M. Ruiz, J. Perelló, L. Velasco, S. Spadaro, and J. Comellas, "An analytical model for GMPLS control plane resilience quantification," *IEEE Commun. Letters*, vol. 13, no. 12, pp. 977–979, Dec. 2009.
- [18] R. Bhandari, *Survivable Networks: Algorithms for Diverse Routing*. Norwell, MA: Kluwer, 1999.
- [19] CPLEX [Online]. Available: <http://www-01.ibm.com/software/integration/optimization/cplex-optimization-studio>
- [20] L. Velasco *et al.*, "GMPLS-based multidomain restoration: Analysis, strategies, policies and experimental assessment," *IEEE/OSA J. Opt. Commun. Netw.*, vol. 2, no. 6, pp. 427–441, Jun. 2010.

Marc Ruiz received the B.Sc. degree in biology from Universitat de Barcelona (UB), Spain, in 2005 and the M.Sc. degree in statistics and operational research from Universitat Politècnica de Catalunya (UPC), Barcelona, Spain, in 2009. He is currently working towards the Ph.D. degree with the Advanced Broadband Communications Center (CCABA).

His research interests include mathematical characterization, planning and re-configuration models of next-generation multilayer optical networks.

Jordi Perelló received the M.Sc. and Ph.D. degrees in telecommunications engineering in 2005 and in 2009 respectively, both from the Universitat Politècnica de Catalunya (UPC), Spain.

Currently, he is an Assistant Professor in the Computer Architecture Department (DAC) at UPC. He has participated in various IST FP-6 and FP-7 European research projects such as EU DICONET, BONE, IST NOBEL 2, e-Photon/ONe+, and COST Action 291. His research interests concern resource management, quality of service issues, and survivability of next-generation optical transport networks.

Luis Velasco received the B.Sc. degree in telecommunications engineering from Universidad Politécnica de Madrid (UPM), Spain, in 1989, the M.Sc. degree in physics from Universidad Complutense de Madrid (UCM) in 1993, and the Ph.D. degree from Universitat Politècnica de Catalunya (UPC), Spain, in 2009.

In 1989 he joined Telefónica de Spain and was involved in the specifications and first office application of the Telefónica SDH transport network. In 2003 he joined UPC, where currently he is an Assistant Professor in the Computer Architecture Department (DAC) and a Researcher in the Advanced Broadband Communications Center (CCABA). His interests include planning, CAPEX/OPEX issues, and survivability in multilayer networks.

Salvatore Spadaro received the M.Sc. (2000) and the Ph.D. (2005) degrees in telecommunications engineering from Universitat Politècnica de Catalunya (UPC), Spain. He also received the Dr.Eng. degree in electrical engineering from Politecnico di Torino (2000).

He is currently an Associate Professor in the Optical Communications Group of the Signal Theory and Communications Department of UPC. Since 2000 he has been a staff member of the Advanced Broadband Communications Center (CCABA) of UPC, and he is currently participating in the DICONET and BONE FP7 EU projects. He has coauthored about 80 papers in international journals and conferences. His research interests are in the field of all-optical networks with emphasis on traffic engineering and resilience.

Jaume Comellas received the M.S. (1993) and Ph.D. (1999) degrees in telecommunications engineering from Universitat Politècnica de Catalunya (UPC), Spain.

His current research interests are optical transmission and IP over WDM networking topics. He has participated in many research projects funded by the Spanish government and the European Commission. He has co-authored more than 70 research articles in international journals and conferences. He is an associate professor in the Signal Theory and Communications Department at UPC, also serving as International Affairs Vice-Dean at the Telecommunications Engineering School (Telecom BCN) of the same university.

Gabriel Junyent received the Ph.D. degree in communications from Universitat Politècnica de Catalunya (UPC), Spain, in 1979.

He was a Telecommunications Engineer with the Universidad Politécnica de Madrid. He has been a Teaching Assistant (UPC, 1973–1977), Adjunct Professor (UPC, 1977–1983), Associate Professor (UPC, 1983–1985), and Professor (UPC, 1985–1989) and has been a Full Professor since 1989. In the past 15 years he has participated in more than 30 national and international R&D projects and has published more than 30 journal papers and book chapters and 100 conference papers.